

Laboratory investigation of the frictional behavior of granular volcanic material

Jon Samuelson ^{a,*}, Chris Marone ^a, Barry Voight ^a, Derek Elsworth ^b

^a Department of Geosciences, Penn State University, University Park, PA 16802, USA

^b Department of Energy and Geo-Environmental Engineering, Penn State University, University Park, PA 16802, USA

Received 14 March 2007; accepted 28 January 2008

Available online 13 February 2008

Abstract

We report on detailed laboratory experiments designed to illustrate the frictional behavior of granular volcanic debris. The materials include pyroclastic flow debris from Soufrière Hills Volcano, Montserrat, and from Stromboli Volcano, Italy, and lahar deposits from Mount St. Helens. Experiments were conducted in a servo-controlled, double-direct shear apparatus under conditions of displacement-control and with monitored temperature and humidity. The effects of loading velocity, normal stress, grain-size range, and saturation state were examined for normal stresses from 0.75 to 8 MPa. The Soufrière Hills debris was sampled in the field using a 2 mm sieve. Samples from Stromboli and MSH represent the original bulk material. The influence of grain-size and size distribution were examined in detail for the Soufrière Hills material for 1) two narrow size ranges (3–4 ϕ , 0.063–0.125 mm; and 0–1 ϕ , 0.5–1 mm), 2) a wide size range (3–0 ϕ , 0.125–1 mm), and 3) the natural size distribution in the range 0–1 mm. These four data sets show remarkably uniform properties: coefficients of residual internal friction varied from 0.62 to 0.64 and coefficients of peak internal friction varied from 0.66 to 0.69, with zero cohesion in each case. For the natural grain-size distribution, we find a small but clear increase in residual sliding friction with increasing slip velocity in the range 10 to 900 $\mu\text{m/s}$, i.e. velocity strengthening frictional behavior. For Soufrière Hills pyroclastic material the coefficient of internal friction changes very little when water saturated. The frictional characteristics were remarkably similar for the three volcanoes. For the natural grain-size distributions, the coefficient of residual internal friction ranged from 0.61 to 0.63 and peak internal friction values ranged from 0.65 to 0.66. Pre-loaded and over-compacted materials sheared at reduced normal stress gave peak coefficients as high as 0.80. Our results imply that granular volcanic debris should often fail via stable creep, but may exhibit stick-slip instability under some conditions.

© 2008 Elsevier B.V. All rights reserved.

Keywords: friction; grain-size distribution; Soufrière Hills; Mount St. Helens; Stromboli

1. Introduction and motivation

Pyroclastic density currents (PDC's) and lahars are two examples of rapid and far-reaching hazards associated with volcanic eruptions. The flow behavior of PDC's and lahars is influenced by inter-particle friction associated with solid particles that come into contact during flow (Iverson, 1997; Cagnoli and Manga, 2004), affecting the velocity of travel and

their reach. Inter-granular friction is of particular importance in understanding the behavior of PDC's as they become degassed and settle to a stop and lahars as they become dewatered. It is also of importance in defining the onset and triggering of instability in the failure of edifices and the failure of lava domes (Voight and Elsworth, 1997; Voight and Elsworth, 2000; Voight, 2000). The intention of this work is not to describe the complex behavior and processes taking place in lahars and pyroclastic flows while they are in full motion, but rather to specifically understand the frictional strength of the material as it might apply to the initiation of a slope failure, or as one of the factors influencing deceleration and stoppage of flows.

Here we present well-constrained experiments (Table 1) to investigate the frictional behavior of material from three

* Corresponding author. 312 Deike Building, University Park, PA 16802. Tel.: +1 814 880 6131; fax: +1 814 863 7823.

E-mail addresses: jsamuels@geosc.psu.edu (J. Samuelson), cjm@geosc.psu.edu (C. Marone), voight@ems.psu.edu (B. Voight), elsworth@psu.edu (D. Elsworth).

Table 1
Experimental conditions and results for samples from Soufrière Hills, Mount St. Helens, and Stromboli volcanoes

Experiment #	Material type	Grain size	Normal stress (MPa)	Shear rate ($\mu\text{m/s}$)	Pre-shear porosity (%)	Relative density (%)	6.5 mm strength (MPa)	10 mm strength (MPa)	15 mm Strength (MPa)	Peak Strength (MPa)	Peak Shown?
p433	SHV P.F.	0.5–1.0	8	10	–	–	5.13	5.19	5.2		n
p504	SHV P.F.	0.5–1.0	2	10	40	150	1.26	1.31	1.34		n
p447	SHV P.F.	0.5–1.0	2	10	–	–	1.22	1.21	1.22	1.3	y
p448	SHV P.F.	0.5–1.0	0.75	10	–	–	0.46	0.45	0.43	0.54	y
p507	SHV P.F.	0.5–1.0	0.75	10	40	150	0.46	0.45	0.44	0.58	y
p467	SHV P.F.	0.063–0.125	8	10	30	200	5.04	5.12	5.12		n
p449	SHV P.F.	0.063–0.125	8	10	–	–	5.07	5.09	4.98		n
p450	SHV P.F.	0.063–0.125	2	10	–	–	1.25	1.19	1.21	1.36	y
p466	SHV P.F.	0.063–0.125	0.75	10	35	170	0.55	0.54	0.51		n
p513	SHV P.F.	0.125–1.0	8	10	30	170	4.93	4.99	5.09		n
p514	SHV P.F.	0.125–1.0	2	10	35	130	1.24	1.2	1.21	1.35	y
p517	SHV P.F.	0.125–1.0	0.75	10	–	–	0.5	0.49	0.45	0.58	y
p596	SHV P.F.	0–1.0	8	10	15	140	4.99	5.01	5.02	5.3	y
p523	SHV P.F.	0–1.0	2	10	20	130	1.21	1.19	1.19	1.27	y
p520	SHV P.F.	0–1.0	2	10	20	130	1.16	1.15	n/a		n
p521	SHV P.F.	0–1.0	0.75	10	20	130	0.49	0.48	0.49	0.56	y
p524	SHV P.F.	0–1.0	0.75 (pre-loaded)	10	20	130				0.6	y
p525	SHV P.F.	0–1.0	8	100	–	–	5.1	5.07	n/a	5.27	y
p529	SHV P.F.	0–1.0	2	100	25	110	1.3	1.25	1.26	1.35	y
p536	SHV P.F.	0–1.0	0.75 (pre-loaded)	100	–	–				1.08	y
p537	SHV P.F.	0–1.0	0.75	100	25	110	0.53	0.53	0.51		n
p528	SHV P.F.	0–1.0	8	900	25	110	5.23	5.15	5.19	5.38	y
p576	SHV P.F.	0–1.0	2	900	30	100	1.27	1.32	1.26		n
p577	SHV P.F.	0–1.0	0.75	900	25	110	0.5	0.5	0.47		n
p543	SHV P.F.	0–1.0	8 (saturated)	10	40	50	5.14	5.1	5.17		n
p545	SHV P.F.	0–1.0	2 (saturated)	10	45	30	1.28	1.26	n/a		n
p544	SHV P.F.	0–1.0	2 (sat, pre-loaded)	10	35	80				1.48	y
p578	SHV P.F.	0–1.0	0.75 (saturated)	10	45	30	0.46	0.44	0.43		n
p557	Stromboli P.F.	0–1.0	8	10	35	160	4.88	4.93	4.89		n
p560	Stromboli P.F.	0–1.0	2	10	35	160	1.22	1.22	1.26	1.31	y
p565	Stromboli P.F.	0–1.0	0.75	10	40	70	0.43	0.42	0.42	0.54	y
p564	Stromboli P.F.	0–1.0	0.75	~53	35	160				0.59	y
p566	MSH Lahar	0–1.0	8 (pre-loaded)	10	–	–				6.05	y
p567	MSH Lahar	0–1.0	8	10	–	–	5.06	5.08	5.09	5.23	y
p568	MSH Lahar	0–1.0	2	10	10	150	1.26	1.25	1.25	1.31	y
p569	MSH Lahar	0–1.0	0.75	10	20	120	0.47	0.47	0.46		n
p570	MSH Lahar	0.5–1.0	8	10	25	–					n
p574	MSH Lahar	0.5–1.0	2	10	25	–					n
p575	MSH Lahar	0.5–1.0	0.75	10	40	–				0.51	y

Relative density was calculated using a technique similar to ASTM test designation D-2049 (1999) (see Appendix A). Only shaded values of peak strength are used for Coulomb failure envelopes.

locations worldwide: pyroclastic debris from Soufrière Hills volcano (SHV), Montserrat, and from Stromboli, Italy, and lahar material from Mount St. Helens (MSH) (Fig. 1). These results provide detailed constitutive data to characterize the evolution of failure and to understand parameters that determine frictional strength. We measure the coefficient of internal friction as a function of mean grain-size and size range, normal stress, shearing rates, and water saturation state.

The control variables used in this analysis: grain-size, saturation state, shearing velocity, and provenance, were chosen in order to explore a wide array of conditions under which granular volcanic material can be expected to fail. Variations in grain size were investigated to understand potential effects of site-source distance. Saturation of the grains was studied to determine if sub-aqueous or rain saturated deposits have different frictional properties than dry deposits. The dependence of frictional strength on shearing rate and transients in rate was

studied to investigate whether the volcanic sediment could host unstable sliding.

2. Geologic background

Stromboli volcano has been erupting almost continuously for thousands of years, and is characterized by frequent mild explosive activity typically taking place every 10–20 min (Guest et al., 2003). Less frequently, small pyroclastic flows also occur in the Sciarra del Fuoco sector collapse scar (Guest et al., 2003), and slope failures and associated tsunami present additional hazards. Much of the Sciarra slope was involved in a large but limited collapse (~10–15 m) in 28–29 December 2002. The submarine part of this body (~ $10 \times 10^6 \text{ m}^3$) failed on 30 December 2002 in a massive slide, which generated a tsunami with an 11-m wave run-up over nearby inhabited areas (Marsella et al., 2004). The slide mass consisted of slabs of

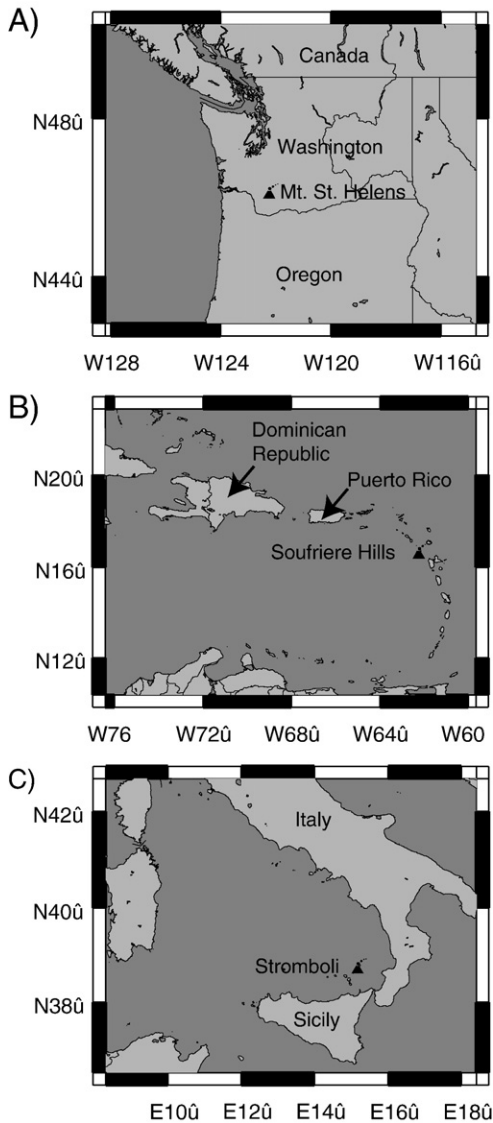


Fig. 1. Locations of samples tested in this study (A) Mount St. Helens volcano, Washington State, USA. (B) Soufrière Hills volcano, Montserrat, West Indies. (C) Stromboli volcano, Italy.

high-K basalt resting on scoria and ash fallout and flowage deposits. A sample from a recent pyroclastic flow deposit at the base of the Sciarra del Fuoco was collected by Barry Voight (BV) in February 2003 and used for our experiments.

At MSH, the 18 May 1980 eruption was triggered by a massive landslide, and accompanied by pyroclastic flows, a plinian eruption column, and lahars derived from snowmelt or from fluidized portions of the debris avalanche. The material used in our experiments was collected by BV from a lahar derived from fluidized parts of the debris avalanche.

Soufrière Hills Volcano on Montserrat has been erupting recently since 1995. The eruptive behavior of SHV has been dominated by the build-up and failure of andesite lava domes, followed in some circumstances by explosive eruptions (Voight and Elsworth, 2000; Druitt and Kokelaar, 2002; Watts et al., 2002). Our studies were performed on a sample from a pyroclastic flow deposit of 8 December 2002, collected by BV at White’s Bottom Ghaut.

The mineralogy of the materials recovered from all three locations is roughly similar. The andesite from Soufrière Hills is dominantly plagioclase with some hornblende, and small amounts of pyroxene, oxides, and glass. Material from Mount St. Helens is similar but with more pyroxene, while the deposits from Stromboli are basaltic, dominantly plagioclase and pyroxene.

2.1. Grain-size distribution

Frictional characteristics may be influenced by the mean grain-size, size distribution, and grain roughness (Sowers and Sowers, 1951; Lambe & Whitman, 1969; Mair et al., 2002; Anthony and Marone, 2005; Knuth and Marone, 2007). Grain-size distribution has been widely applied to classify pyroclastic deposits; we use the methods of Inman (1952), and compare our samples to the classification created by Walker (1971) for typical pyroclastic deposits. The three material types used in this study are relatively well-graded (Fig. 2), comprising a broad range of grain-sizes but with no gaps (Das, 2002).

All of the material was sieved using stacked sieves of 0.063, 0.125, 0.25, 0.5, and 1 mm mesh size (4, 3, 2, 1, and 0 ϕ). For the Stromboli material a 3.36 mm (−1.75 ϕ) sieve was added to the top of the stack, and for the Mount St. Helens’s material, 3.36 mm, 6.35 mm (−2.67 ϕ), and 50.8 mm (−5.67 ϕ) sieves were added. The sieving was conducted both to characterize the bulk material and to separate the size ranges for specialized testing. The SHV sample was previously sieved in the field, using a 2 mm sieve size (Fig. 2). Samples from Stromboli and MSH are representative of the original bulk material.

Using the particle size distribution curves we calculate the sorting σ_ϕ and median diameter Md_ϕ parameters (Inman, 1952). For SHV, σ_ϕ is 2.01 and Md_ϕ is 1.23 ϕ (0.43 mm), such

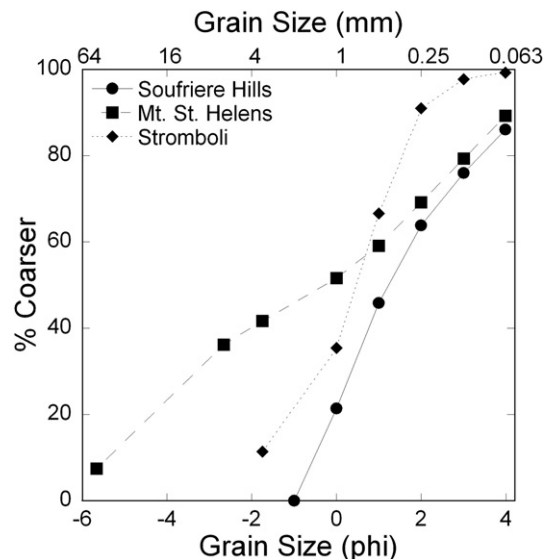


Fig. 2. Grain-size distributions for the materials tested. The Soufrière Hills pyroclastic flow material was sieved at 2 mm in the field and therefore the distribution curve is truncated at 2 mm. The grain-size distributions of the Mount St. Helens lahar and Stromboli pyroclastic flow materials are not truncated. Note that the Mount St. Helens and Soufriere Hills materials do not reach 100% because the grain-size scale does not go to zero.

values are typical of pyroclastic deposits (Walker, 1971). The Md_{ϕ} of the Stromboli material was 0.48ϕ (0.72 mm), and the σ_{ϕ} 1.57. The lahar deposit from MSH is coarser than the other samples $Md_{\phi} = -0.25$ (1.19 mm) and $\sigma_{\phi} = 4.13$. These grain-size characteristics are similar to the pyroclastic flow deposits discussed by Walker (1971), but are typical also of debris avalanches and lahars.

The grain-size distribution of the Stromboli material most properly fits within the realm of a pyroclastic fall (Walker, 1971). The Stromboli material is different from both the SHV and MSH materials in that it lacks any significant fraction of fines. Only ~2.3 wt.% of the Stromboli material is <0.125 mm (3ϕ), whereas the SHV and MSH materials have >21 wt.% finer than 0.125 mm.

3. Sample preparation and experimental technique

Uniform experimental conditions were applied, including magnitudes of normal stresses, and shear rates; with contrasting grain-size ranges. These conditions were applied to determine the principal similarities and differences between the volcanic materials from several sites.

Our experiments were run in a servo-controlled biaxial double-direct shear configuration (e.g., Anthony and Marone, 2005). In this arrangement two layers of sediment are sandwiched between 3 hardened steel forcing blocks (Fig. 3). The two identical side blocks have dimensions $10 \times 10 \times 2.54$ cm, and the larger center block has dimensions $15.06 \times 10 \times 3.86$ cm. The faces of the forcing blocks in contact with the sample are cut with 0.8 mm deep grooves at a spacing of 1 mm perpendicular to the direction of shear. This establishes coupling between the sheared material

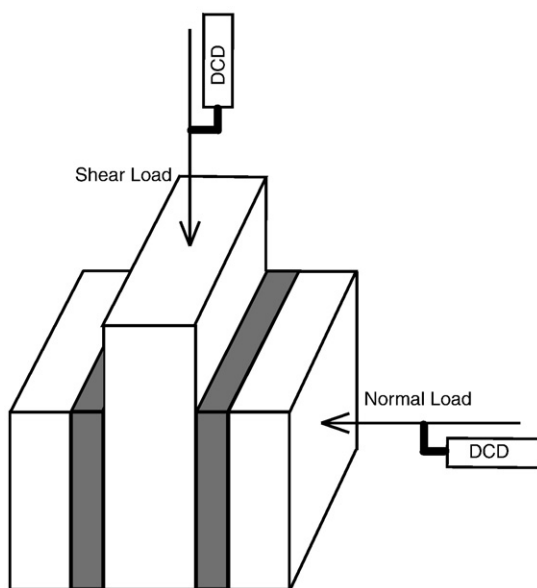


Fig. 3. Schematic illustration of the double-direct shear friction configuration showing the orientation of the sample set-up and the direction of applied normal and shear stresses.

and the forcing blocks and ensures that shearing occurs within the layer and not at the boundary.

Samples were prepared by ringing the side blocks with a 5-mm deep “fence” of cellophane tape, and filling the so-contained area with test material. The block was then placed in a leveling jig and material spread to an even thickness over the block. The two side blocks were adhered to the center block with tape to provide enough mechanical strength for handling during set-up in the testing apparatus. Steel guide plates were then fastened onto the front/back of the sample to prevent loss of material during shear. Copper shims were added to the bottom of the sample to prevent leakage from the bottom during shearing (Fig. 3).

In order to maintain a large ratio between the initial layer thickness and the maximum grain-size, which ensures that the layer is matrix supported rather than clast supported, only material smaller than 1 mm was used experimentally. There is a possibility that altering the natural field grain-size distribution to include only those materials smaller than 1 mm could influence the frictional strength of the material. However, the results of this work, and other studies (e.g., Marone and Kilgore, 1993; Mair and Marone, 1999), suggest that although the mean grain-size may have an effect on the second-order frictional behavior, the overall frictional strength is independent of grain size.

Once placed into the testing apparatus, normal and shear stresses were applied by servo-controlled hydraulic rams. Experiments were conducted by first applying the desired normal load (0.75, 2, or 8 MPa); the normal stress was then held constant using servo-control during shear. The center block of the double-direct shear arrangement was driven down through the layers, shearing the granular layers, at a constant velocity (here 10, 100, or 900 $\mu\text{m/s}$) (Fig. 3). Normal and shear stresses on the layers were measured using load cells accurate to 0.01 MPa, displacements were measured by direct current displacement transducers (DCDTs) accurate to 0.1 μm . Maximum shear displacement in any one experiment was ~20 mm.

The limits of the normal stresses we used correspond to granular deposits roughly 40–400 m thick. Limitations of the experimental apparatus and the geometry of our configuration prevented us from running tests at lower normal stresses.

The mass of the granular layers was measured prior to each experiment, and along with a measured mineral density of the material, the total volume of granular solid material was calculated. Porosity was measured as the difference between the total space enclosing both layers, and the volume of granular solids comprising the layers. Calculated porosity after application of the normal load but before the onset of shear is given in Table 1. These calculations were fairly crude although they appear mostly consistent, but with considerable uncertainty in a few cases. The measured values were rounded to the nearest 5%. Relative density, D_r , (Lambe and Whitman, 1969; Das, 2002) was measured using a technique similar to ASTM D-2049 devised for engineering purposes. Measurement of porosity changes during shear are derived from the continuous measurement of layer thickness after correcting for shear induced geometric thinning of the layer (e.g., Scott et al., 1994).

4. Results

Results from a typical shear experiment are shown in Fig. 4. This sample was sheared at 8 MPa normal stress and exhibits a distinct peak shear stress. In many cases at a normal stress of 8 MPa, the ultimate or residual strength (Lambe and Whitman, 1969) was reached by a gradual “hardening,” without a peak stress. Because of this behavior we chose to measure the shear strength of the material at displacements of 6.5, 10, and 14 mm to produce Coulomb strength envelopes. Each Coulomb plot includes all of the data. Measurements of changing Coulomb behavior as a function of increasing displacement are not included here. Coulomb plots of the peak strength are also provided in a few cases.

We conducted experiments with a wide variety of grain-size conditions, shear velocities, and material types. The SHV material was chosen for detailed studies of certain parameters and in these cases we used a standard shear velocity of 10 $\mu\text{m/s}$ and material <1 mm in diameter, unless otherwise noted. The influence of grain-size was investigated by sieving and reconstituting mixtures of grains. The influence of relative density was studied under a limited range of conditions.

4.1. Effect of varying grain-size range

We conducted experiments on the natural grain-size distribution of SHV material finer than 1 mm; a restricted size range from 0.125 to 1 mm; and two narrow grain-size ranges, one with relatively large grain-size of 0.5 to 1 mm, and a second with a smaller grain-size of 0.063 to 0.125 mm (Fig. 5). A histogram plot of grain-sizes accompanies SEM images of the four different grain-size classes tested, in Fig. 5.

These experiments were conducted at a constant shearing velocity of 10 $\mu\text{m/s}$ and normal stresses of 0.75, 2, and 8 MPa.

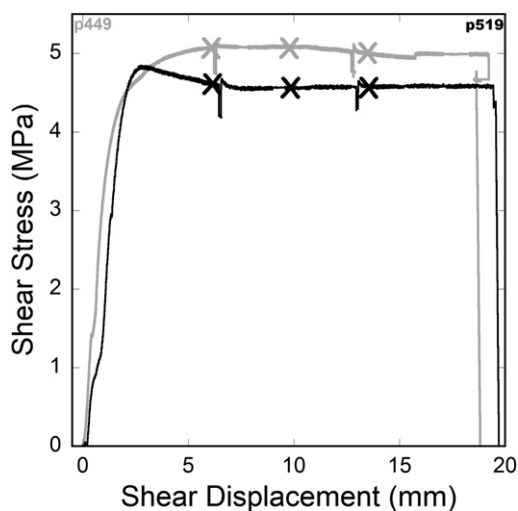


Fig. 4. Results of a typical shear test. \times 's at 6.5, 10, and 14 mm displacement mark the locations where shear stresses are recorded for use in determining the Coulomb failure envelopes. Sharp decreases in shear stress at \sim 6.5 and 13 mm are a result of pauses in shearing rate, to reset the vertical DCDT. The gray line represents a test conducted on the 0.063–0.125 mm SHV pyroclastic material at 8 MPa, and the black line represents a test on 0–1 mm SHV pyroclastic material at 8 MPa.

Results were used to determine a Coulomb failure envelope and coefficient of internal friction (μ_i) for each material

$$\tau = C + \mu_i \sigma, \quad (1)$$

where τ is shear stress, σ is the applied normal stress, and C is cohesion. Because we are working with a granular material at relatively low normal stress, we assumed that cohesion is zero in all experiments though it is possible that there is an apparent cohesion due to grain packing. Our data show negligible values of C , but for consistency we forced curve-fits for Coulomb envelopes through zero. Shear strength values used in the Coulomb analysis were measured at 6.5, 10, and 14 mm displacement.

Coulomb envelopes for our experiments (Fig. 6) indicate that the narrowest grain-size ranges, 0.063–0.125 mm and 0.5–1 mm, show the highest strengths with coefficients of residual friction of 0.63 and 0.64 respectively. The initial pre-shear porosities calculated for these tests on well-sorted material were about 30–35% (D_r : >170%), and 40% (D_r : 150%), respectively. Note that our D_r values can exceed 100%. This indicates a packing more dense than the theoretical minimum porosity values measured by the simplified ASTM procedure. We suggest that this discrepancy may reflect mainly the difference between the \sim 0.02 MPa normal load applied in our “standard” calibration tests, and the 0.75–8 MPa normal loads applied in the shear tests. The wider grain-size ranges show a slightly smaller coefficient of residual friction of 0.62, with initial porosities ranging from 30–35% (D_r : >130%) for 0.125–1 mm material, and generally 15–25% (D_r : 110–140%) for the natural gradation. In the latter instance, the tests at <2 MPa had initial porosities of \sim 20–25% (D_r : 110–130%), whereas increased normal load at 8 MPa increased compaction, with porosities of \sim 15–25% (D_r : 130–140%). The peak strength data show a different trend. The coefficient of peak friction for the 0–1.0 mm material is the lowest of the group at 0.66, increasing to 0.67, 0.68, and 0.69 for the 0.5–1.0, 0.063–0.125, and 0.125–1.0 mm samples respectively (Table 1).

These experiments show good reproducibility with the largest difference in shear strength between duplicate runs of the same experimental parameters being \pm 0.05 MPa.

4.2. Effect of sample saturation

Pore pressure has a significant effect on the frictional strength of materials (Hubbert and Rubey, 1959; Voight, 1976), and there is evidence in clay rich materials that the mere presence of water has a weakening effect on strength (Horn and Deere, 1962; Wiebe et al., 1998; Ikari et al., 2007). We do not examine the effects of elevated pore pressure in this study, but rather examine potential effects of saturation on the strength of the SHV material, excluding drainage related behavior with augmented or undrained pore fluid pressures. In this suite of experiments, only the natural grain-size range (<1 mm) was used. All tests were conducted at a shear velocity of 10 $\mu\text{m/s}$ and at normal stresses of 0.75, 2, and 8 MPa.

We conducted saturated experiments using a latex sheath, which was folded around the sample and filled with water at room temperature. The sample was then left to fully saturate for

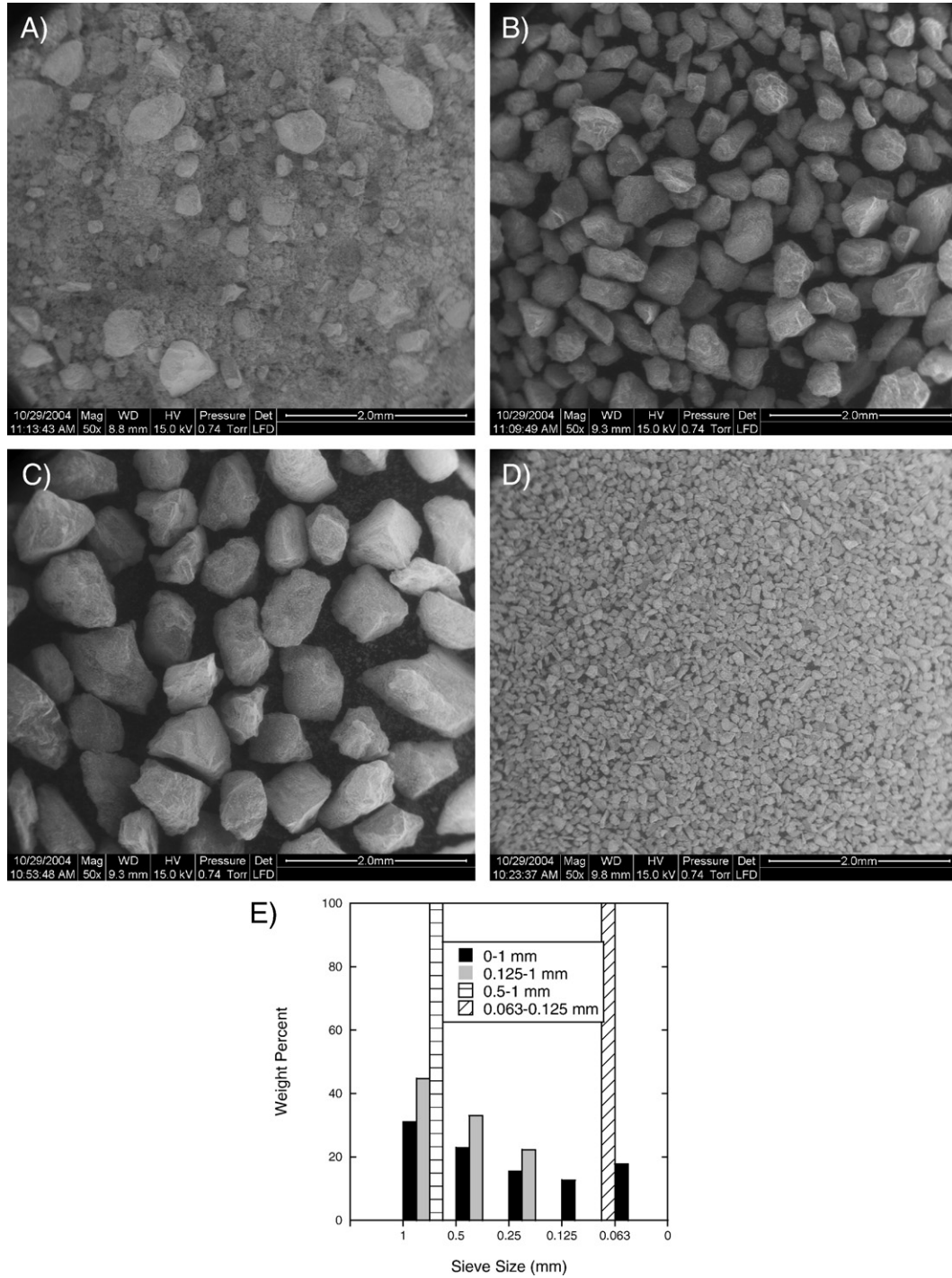


Fig. 5. Grain-size distributions of materials recovered from Soufrière Hills volcano. SEM photos (A–D) are all at 50× magnification with a scale bar length of 2 mm. (A) All material passing a 1 mm sieve. (B) All material coarser than 0.125 mm and finer than 1 mm. (C) Material finer than 1 mm and coarser than 0.5 mm. (D) Material finer than 0.125 mm and coarser than 0.063 mm. (E) Histogram showing the abundance of grain-size ranges in experimental samples.

approximately 20 min. The experiment was then run as normal. The Coulomb failure envelopes showing the difference between the dry and saturated materials with natural grain-size range (Fig. 7) suggest a very small strength difference between materials in the two states. The saturated Soufrière Hills pyroclastic material shows a slightly larger coefficient of residual internal friction of 0.64 than the dry material (0.62). A

possible explanation for this is the potential generation of negative pore pressures in the sample, increasing the effective stress and therefore frictional strength. However, the initial porosities for these two sets of experiments were different. For the wet material the porosity was about 35–45% (D_r : 30–80%), greater than the 15–25% (D_r : 110–140%) for the dry case, suggesting an initial loosening of grain structure by water percolation. In any case

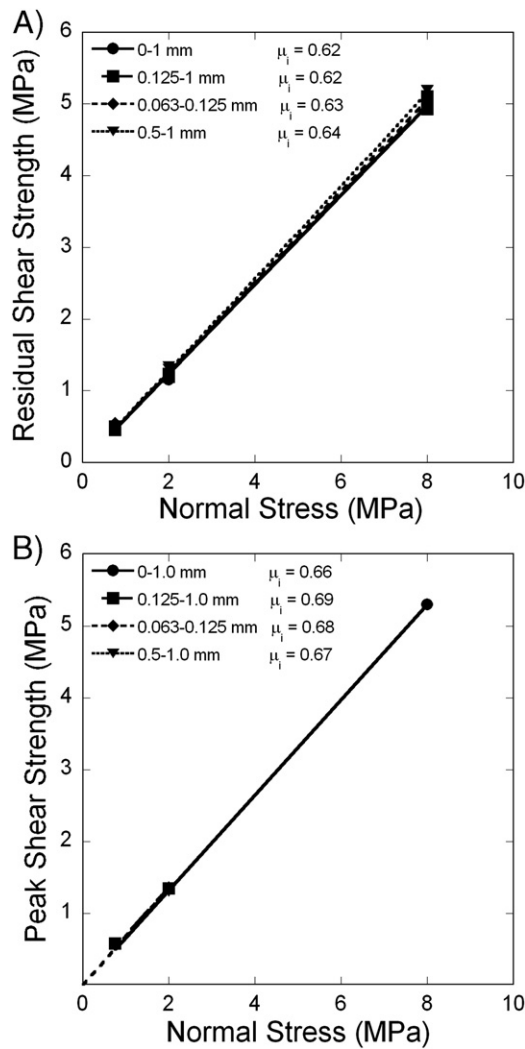


Fig. 6. Coulomb failure envelopes for the four different grain-size ranges of Soufrière Hills pyroclastic material. (A) Envelopes produced using residual shear strength. (B) Envelopes produced using available peak strength data. Tests were conducted at a shear rate of 10 $\mu\text{m/s}$ and at normal stresses of 0.75, 2, and 8 MPa. Note that in both panels several data points lie over one another. See Table 1 for complete data set.

these tests provided our only data for $D_r < 100\%$, indicating a pronounced effect of water on initial test conditions. A visual attempt was made to verify saturation after completion of the experiment, but there is the potential that shearing aided the saturation; also we cannot exclude the possibility of very minor pores of air within the sample that could have increased local effective stress through capillary effects. The main conclusion is that the coefficient of residual friction changes very little, if at all, as a result of water saturation.

4.3. Effects of changing shear velocity

Shearing velocity has been shown to have an important effect on the shear strength of materials, particularly for gouges representative of mature faults (e.g., Mair and Marone, 1999). This type of frictional velocity dependence has also been used to

explain seismic phenomena associated with the stick-slip motion of a dacite plug being extruded at Mount St. Helens during the 2004–2005 eruptive phase (Iverson et al., 2007; Moore et al., 2007). Rate and state friction behavior is examined by a velocity stepping procedure, where load point shear velocity is either successively incremented, or decremented, relative to the steady shear velocity, within a single test (Marone, 1998; Mair and Marone, 1999). Such experiments are conducted by shearing the sample until a residual value of shear stress is obtained. The load point sliding velocity is then increased and a new local peak in the shear stress is observed followed by decay to a new steady-state or residual shear stress for the new velocity. If the new background shear stress is higher than at the slower velocity the material is said to be velocity strengthening, if lower, velocity weakening. This is important, especially within the context of faulting, because a velocity weakening material has the potential to host so-called “stick-slip” sliding whereas a velocity strengthening material would not display such behavior.

In an effort to limit any influence on frictional strength from a change in grain-size distribution due to grain fracture during shear, a series of experiments was run, each at constant velocity. Shear velocities of 10, 100, and 900 $\mu\text{m/s}$ were used in our experiments. Tests were, once again, conducted on the natural grain-size distribution < 1 mm for the SHV material. Initial porosities for the rapidly sheared samples were comparable to those sheared at the standard rate, i.e. about 25% (D_r : 110%) for normal stress < 2 MPa, and $\sim 15\%$ (D_r : 140%) at 8 MPa. Three separate Coulomb failure envelopes (Fig. 8A) show that with each increase in velocity there was a small, but resolvable, increase in frictional strength. At 10 $\mu\text{m/s}$ we see a coefficient of residual internal friction of 0.62, whereas at 100 and 900 $\mu\text{m/s}$ we see coefficients of 0.64 and 0.65 respectively. Fig. 8B illustrates the increase in frictional strength with increased sliding velocity. Examination of grains post-test shows that significant

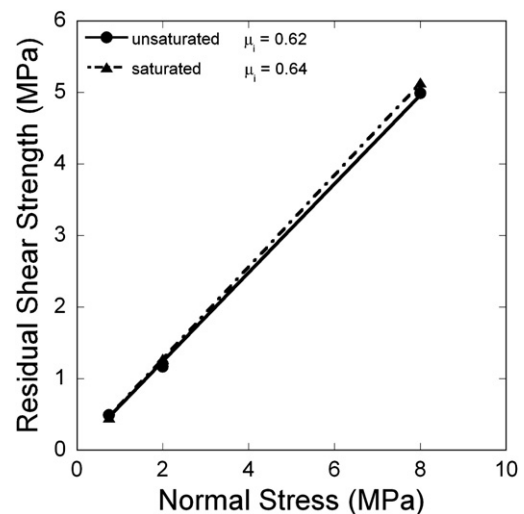


Fig. 7. Coulomb failure envelopes describing the failure criteria for a natural grain-size distribution (all materials < 1 mm) of Soufrière Hills pyroclastic flow material in both saturated and unsaturated states. Tests were conducted at a shear rate of 10 $\mu\text{m/s}$ and at normal stresses of 0.75, 2, and 8 MPa.

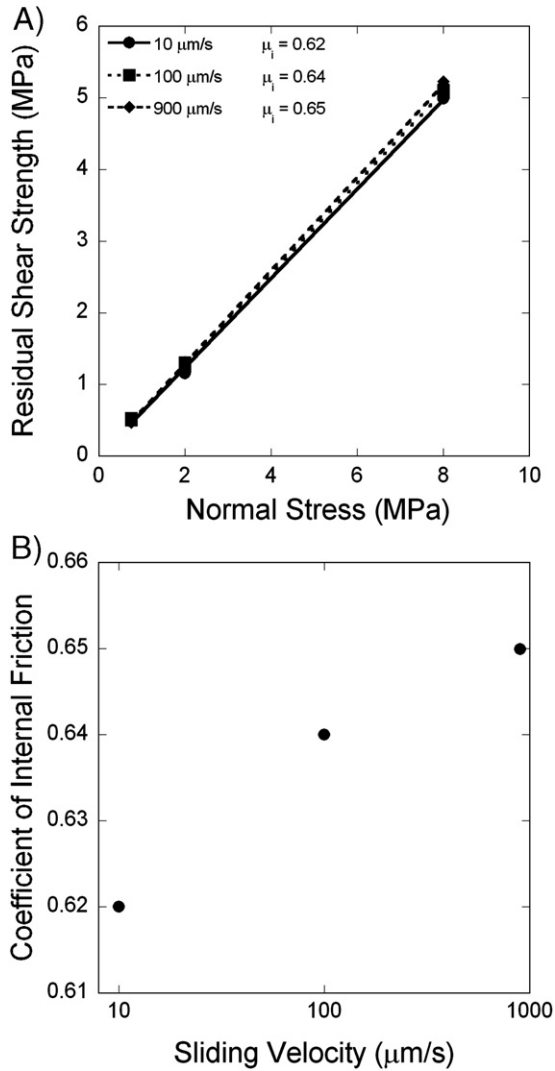


Fig. 8. (A) Coulomb failure envelopes for a natural grain-size distribution (all materials < 1 mm) of Soufrière Hills material for shear velocities of 10, 100, and 900 μm/s. (B) The sliding frictional strength of the layer is shown to increase with an increasing sliding velocity.

grain fracturing occurred during shear. This was confirmed by sieving the sample both pre- and post-test, as illustrated in Fig. 9, which shows several percent reduction in coarse fraction, and several percent increase in fines.

4.4. Friction tests on materials from other volcanoes

To test the possible variation in frictional strength of materials from differing geographic localities, we conducted experiments on pyroclastic material from Stromboli volcano, and lahar material from MSH in addition to the pyroclastic material from SHV. Tests were conducted at 10 μm/s and at normal stresses of 0.75, 2, and 8 MPa.

As with the principal suite of experiments conducted on SHV samples, the Stromboli and MSH materials were sieved and only the < 1 mm fraction was tested. Grain-size analysis (Fig. 10) shows that the gradations of the SHV and MSH samples are similar, whereas the material from Stromboli has a

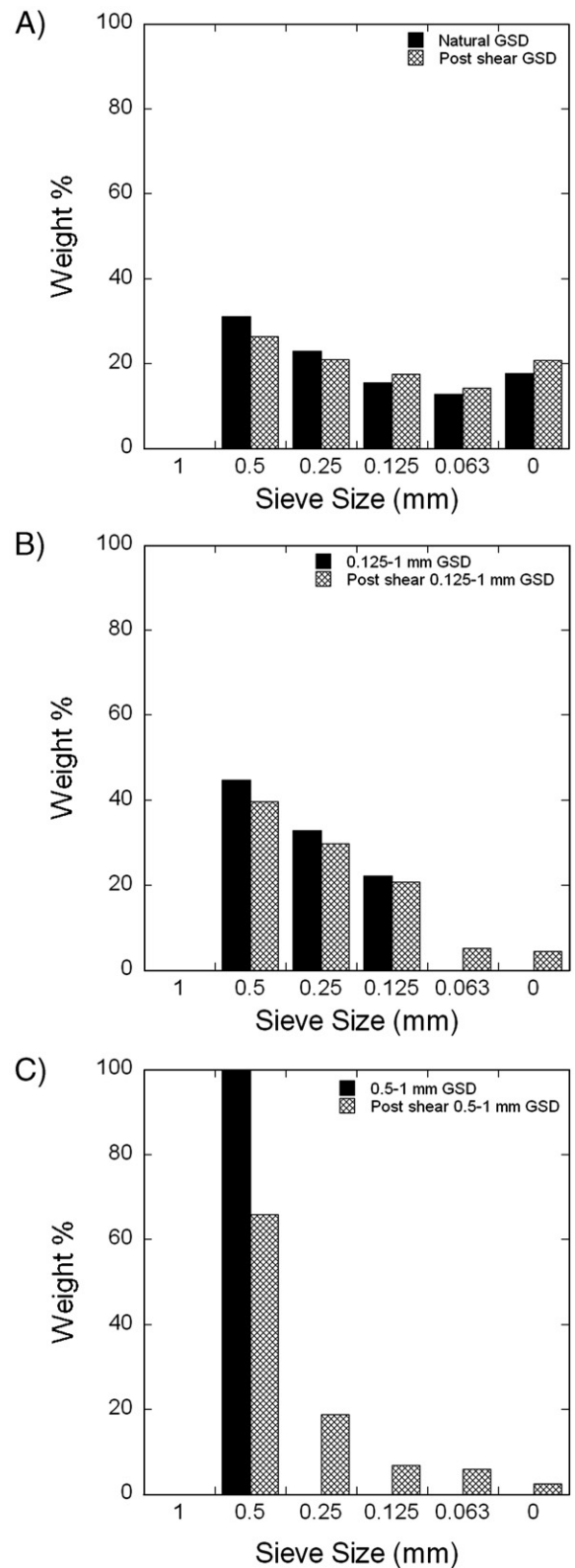


Fig. 9. Grain-size distribution of the natural SHV sample (< 1 mm) shown before and after shearing. Experiments shown were run at 0.75 MPa normal stress and at a shear rate of 10 μm/s. (A) Experiment p521 with natural grain-size distribution. (B) Experiment p517 with initial grain-size distribution of 0.125–1 mm. (C) Experiment p507 with initial grain-size distribution of 0.5–1 mm.

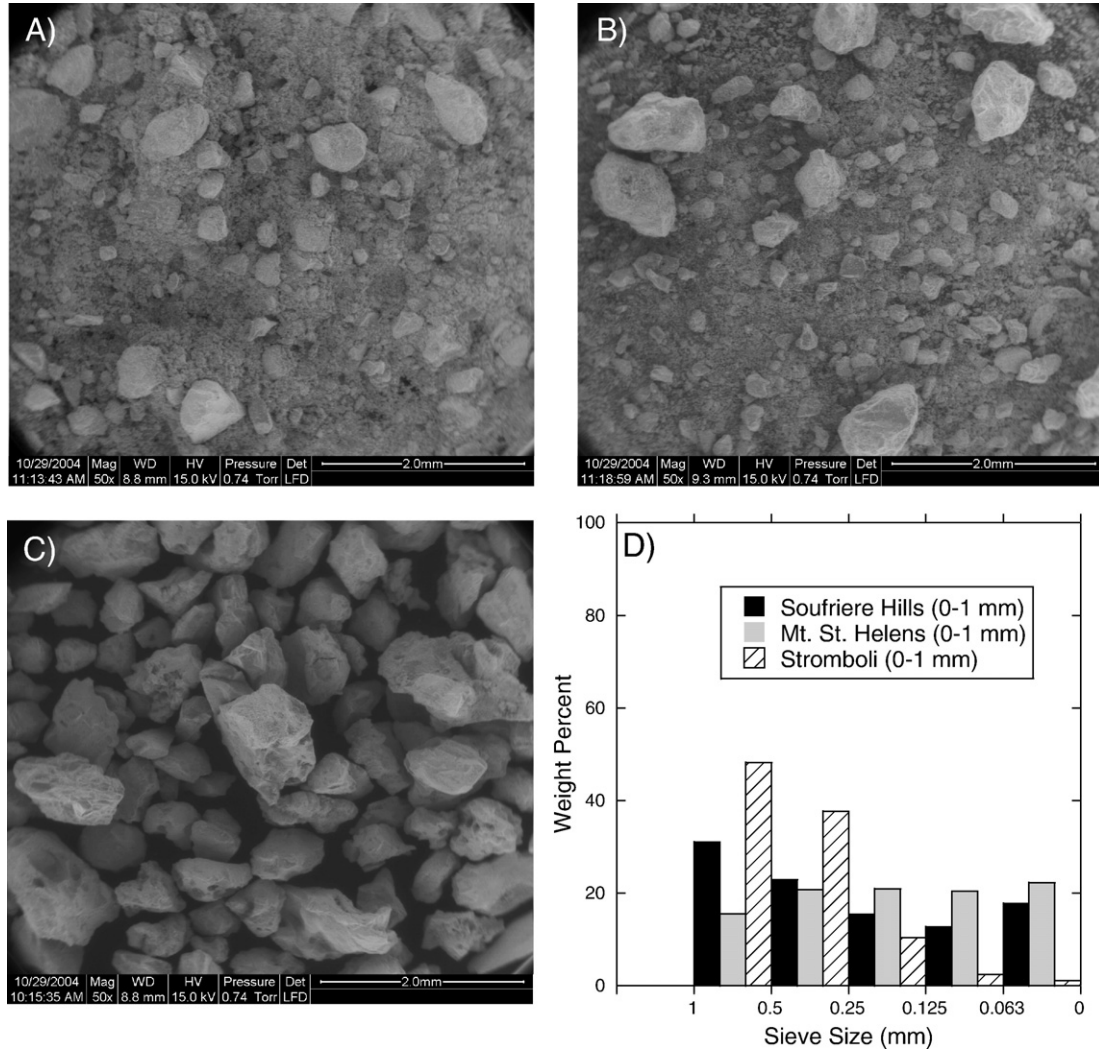


Fig. 10. Grain-size distributions of materials from Soufrière Hills, Stromboli, and Mount St. Helens. SEM photos (A–C) are all at 50× magnification with a scale bar length of 2 mm. All materials are the natural size distribution that passed a 1 mm sieve. (A) Soufrière Hills pyroclastic material (B) Mount St. Helens’s lahar material (C) Stromboli pyroclastic material (D) Histogram plot of the grain-size distribution of the materials.

significantly smaller fraction finer than 0.125 mm. The initial porosities for the natural-graded Stromboli material were around 35–40% (D_r : 70–160%), whereas the naturally graded MSH lahar sample had porosities of roughly 10–20% (D_r : 120–150%), and 20–40% porosity for the 0.5–1 mm fraction.

The results of our experiments are shown in the form of Coulomb failure envelopes (Fig. 11). The material from Stromboli has the lowest coefficient of residual internal friction, 0.61, and the SHV and MSH materials yielded slightly larger residual friction coefficients of 0.62 and 0.63, respectively. All Stromboli tests at load <2 MPa showed a peak strength as did several of the MSH tests (Table 1). The peak strength coefficients for our tests of MSH and Stromboli material were 0.65 and 0.66 respectively (Fig. 11). For the sparse data on pre-loaded tests, the SHV data suggest a peak friction coefficient of 0.80, and MSH data gave a peak coefficient of 0.76.

As with the experiments on SHV material of variable grain-size, the limited peak strength data available for this suite of experiments suggests little quantifiable difference in the frictional strength of material from the three separate localities.

4.5. Effect of pre-loading on shear resistance

The materials examined in this suite of experiments exhibited classical frictional response (Lambe and Whitman, 1969; Das, 2002). Pre-loaded sediments, in which the specimen is initially loaded to a normal stress in excess of the normal stress applied during shear, show a peak frictional strength higher than that of a “normally consolidated” sediment, consistent with previous work (Terzaghi and Peck, 1948). For our standard experiments, the normal stress applied during shear is also the maximum normal stress for the stress history of that specimen (Fig. 12). The data shown are from experiments conducted on MSH lahar material. The thin lines show an experiment conducted under standard conditions with a normal stress of 8 MPa and a driving velocity of 10 μm/s. The thick lines represent an experiment that was conducted under the same conditions, but initially subjected to a normal stress of approximately 50 MPa, held for a few minutes and then reduced to 8 MPa. In each sample, the frictional resistance builds as the

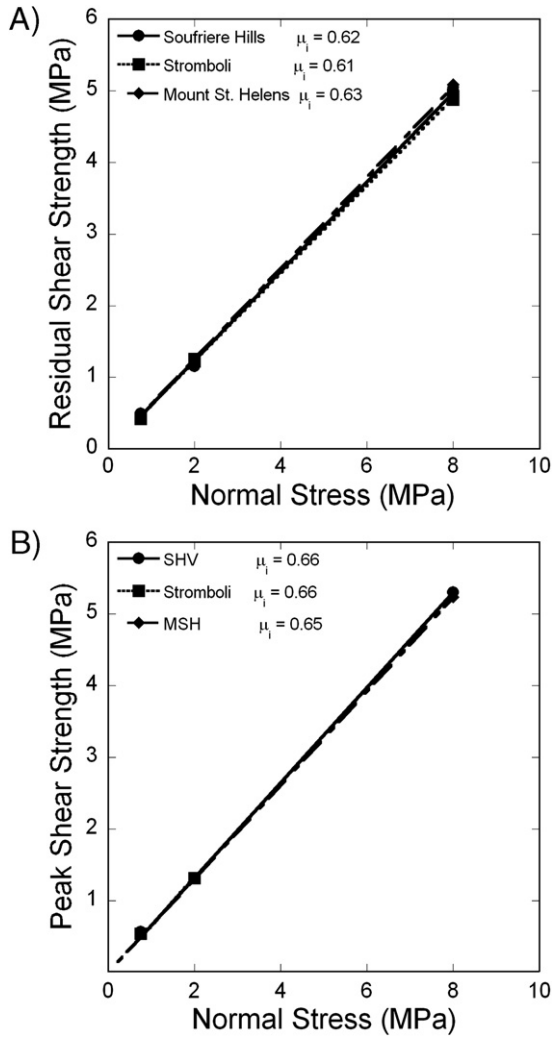


Fig. 11. Coulomb failure envelopes for a natural grain-size distribution (all material <1 mm) of Soufrière Hills pyroclastic, Stromboli pyroclastic, and Mount St. Helen’s lahar materials. (A) Results from the residual shear strength data. (B) Results from available peak shear strength data. Measurements of shear strength were made at a shear rate of 10 μm/s and at normal stresses of 0.75, 2, and 8 MPa to construct the failure envelopes. Note that in both panels several data points lie over one another. See Table 1 for complete data set.

layer is sheared. However, the pre-loaded sample (with unmeasured initial porosity) exhibits a pronounced peak in shear strength, and a line drawn through this point on a Coulomb plot suggests an apparent peak friction coefficient of 0.76. After the pronounced peak, the shear strength of the pre-loaded sample decays to a background level that is nearly identical to that of the normally loaded sample, for which the residual coefficient of friction is 0.63.

Also shown in Fig. 12 are layer thickness data for normal and pre-loaded samples. The thin line (normally consolidated experiment) shows a rapid decrease in layer thickness in the first 1 mm of displacement followed by a constant rate of layer thinning, which represents geometric thinning due to smearing of the layer (e.g., Scott et al., 1994). The layer thickness of the pre-loaded sample is fairly static for the first 1 mm of displacement, then dilating, and finally thinning steadily for the

duration of the experiment, also due to geometric smearing of the layer. The peak of the shear stress for the over-consolidated sample is coincident with the maximum rate of change of the layer thickness during dilation. This congruence between the peak shear strength and peak dilation rate may be understood in the context of the work expended in shearing.

The total work (W) expended in shear can be expressed as

$$W = W_f + PdV \tag{2}$$

where W_f is the work done against friction and PdV is the work done against the normal load P by the dilation of the layer through a change in volume dV (Bishop, 1954; Rowe, 1962). We follow the notation of Marone et al. (1990) and normalize terms with respect to the layer volume (V) to yield the work done per unit volume, as,

$$\frac{W}{V} = \frac{W_f}{V} + P \frac{dV}{V}. \tag{3}$$

The value dV/V is the volumetric strain $d\theta$. Acknowledging that work is equal to force times displacement, Eq. (3) can be simplified to read:

$$\tau d\gamma = \tau_f d\gamma + \sigma_n d\theta, \tag{4}$$

where τ is the applied shear stress, τ_f is the component of shear stress due to friction and σ_n is the applied normal stress. This equation can be further simplified by dividing through by $d\gamma$ and σ_n the result of which is:

$$\mu = \mu_f + \frac{d\theta}{d\gamma}. \tag{5}$$

For our configuration, in which nominal frictional contact area is constant, the term $d\theta/d\gamma$ can alternatively be described as dh/dx which is simply the change in layer thickness with

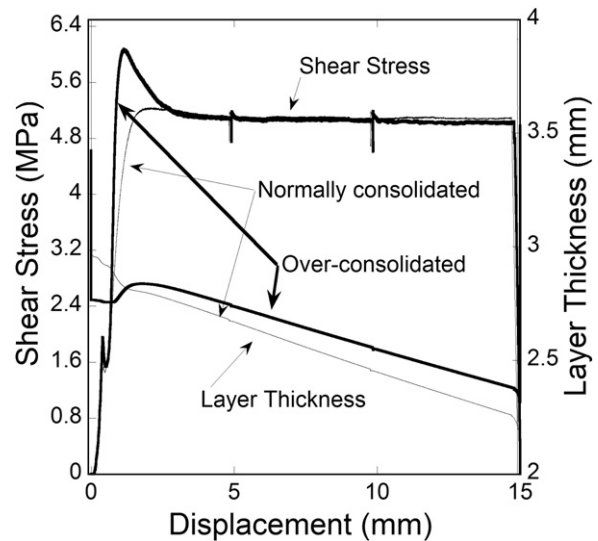


Fig. 12. Evolution of shear stress and layer thickness as a function of displacement for a sample of the natural grain-size distribution (<1 mm) of Mount St. Helens lahar. The results contrast response for a sample “normally consolidated” at a normal stress of 8 MPa (p567) and sheared at 10 μm/s (thin black line) with the same material pre-loaded to ~50 MPa (p566), then also sheared at a rate of 10 μm/s under a normal stress of 8 MPa (thick black line).

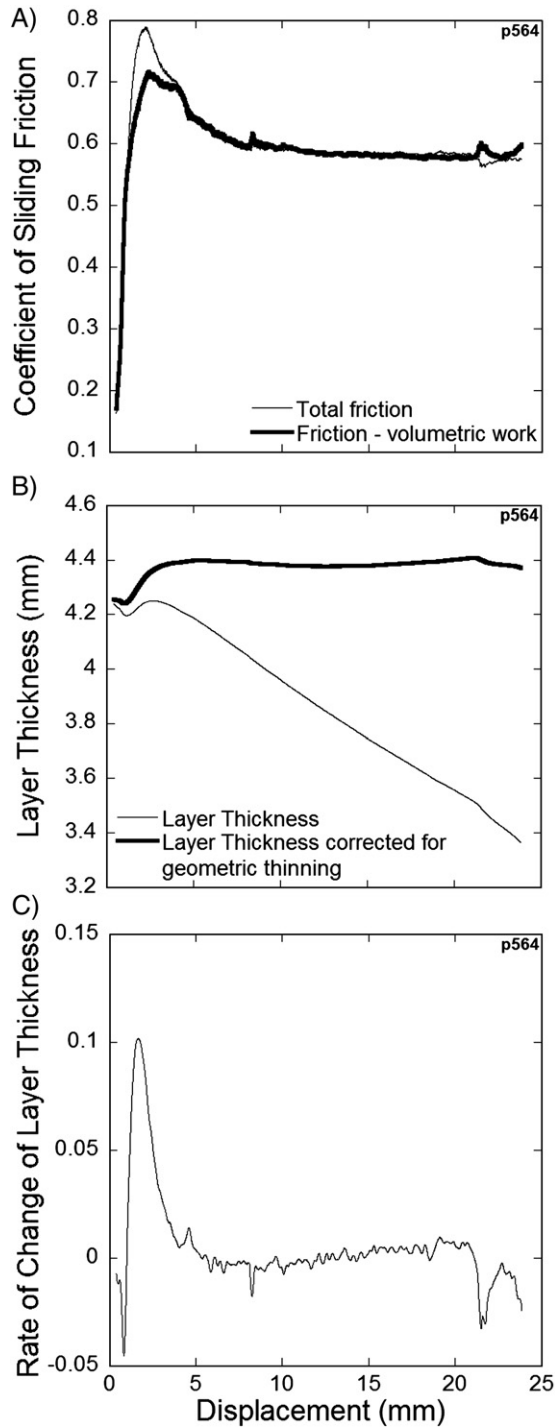


Fig. 13. The evolution of test parameters in pyroclastic material from Stromboli, confined at 0.75 MPa and sheared with a velocity of $\sim 53 \mu\text{m/s}$. (A) Intrinsic friction of the material (heavy black line) and total friction (light black line). (B) Measured thickness of the layer (light black line) and layer thickness corrected for geometric thinning (heavy black line). (C) Rate of change of the layer thickness. Note correlation between peak rate of layer dilation and peak frictional strength.

shear once corrected for thinning associated with the shearing geometry. This quantity is measured directly in our experiments. Eq. (5) states that we should see the largest value of shear stress where the rate of change of layer thickness is maximum.

Fig. 13 shows several plots from the Stromboli sample at 0.75 MPa normal stress, which reinforce the ideas set forth in Eqs. (2)–(5). The top panel shows both μ and μ_f from Eq. (5), the middle panel shows the evolution of layer thickness, and the bottom panel shows the rate of change of the layer thickness. As predicted by Eq. (5), the coefficient of internal friction (μ) is at a maximum when the layer is dilating at the maximum rate. The initial porosity for the Stromboli samples was about 35% (D_r : 160%).

5. Discussion

For shear of a granular material, with all other factors equal, the material with the widest grain-size range is expected to exhibit the greatest strength (Lambe and Whitman, 1969; Das, 2002). This has been rationalized by considering that particles from the finest end of the grain-size range will fill the gaps between the largest particles and add to the strength of the material (Terzaghi and Peck, 1948; Sowers, 1979). This effect may increase the coefficient of friction. On the other hand, the infill effect may require less energy for dilation, thus decreasing frictional strength (Morgan and Boettcher, 1999). These observations may be tested, and the tests reported here show only small differences in strength coefficients for samples with wide variation in size range, and also minor effects where two samples differ only in their mean grain-size, which is the case for a subset of our experiments, grain-size ranges of 0.063–0.125 and 0.5–1 mm. The peak shear strengths are mostly affected by dilation, and the peak strengths for various size gradations of SHV material at 0.75 MPa are similar. Comparably, in experiments conducted at 5 MPa normal stress, Mair et al. (2002) found that a wide versus a narrow grain-size range had little effect on the frictional strength of spherical glass beads. With quartz grains the grain-size range has been shown to be important with well-graded samples showing a significant increase in coefficient of internal friction compared to samples of uniform grain-size (Terzaghi and Peck, 1948; Sowers, 1979).

The current suite of experiments exhibited significant grain fracture at all normal stresses (Fig. 9) consistent with the work of Scott et al. (1994). This means that shear induced comminution reduced, to some extent, the differences in the grain-size distribution of our materials — with a corresponding effect on the shear strength. Some of this fracturing could have occurred during imposition of normal loads, perhaps explaining the commonly small initial porosities in comparison with the minimum porosities achieved in relative density tests. The difference in frictional strengths corresponding to the isolated effect of the grain-size range appears to have been small. Shear experiments on similar volcanic materials have exhibited a wider range of coefficients of internal friction than reported here (Meyer et al., 1983; Voight et al., 1983; Major et al., 1997; Voight et al., 2002; Apuani et al., 2005), but most data are not significantly different than our results. Experiments on the materials from MSH suggest a range of coefficients of friction from 0.60 to 0.97 (Meyer et al., 1983) and from 0.78 to 0.93 (Voight et al., 1983), and more consideration was given to peak strengths, as well as residual strengths. These experiments were conducted in a less-stiff testing

apparatus and at lower stresses (1 MPa, and 2.8 MPa maximum normal stresses, respectively, in the above references) than ours.

Experiments conducted on material from SHV (Voight et al., 2002) suggested coefficients of internal friction ranging from 0.59 to 0.70 and as low as 0.05 in the case of a very clay rich sample. This range gives strengths for granular material very similar to those reported here (0.62–0.69).

Observed increases in shear strength with shear rate are congruent with the general observation that grain fracture is a rate strengthening process (Marone, 1998). Experiments designed to illuminate the importance of particle angularity (Terzaghi and Peck, 1948; Sowers, 1979; Mair et al., 2002; Anthony and Marone, 2005) on the frictional characteristics show an increase in frictional strength for angular particles compared to smooth particles. The coefficients of internal friction reported for angular grains in a well-graded sample can be as high as 1, whereas our samples with less extreme angularity showed coefficients of the order of 0.6–0.7.

The relatively small increase in the coefficient of residual internal friction resulting from water saturation indicates that welding of the grains did not occur, which of course is not expected at the temperature and timescales of our experiments. Prior results have indicated time-dependent strengthening, due to welding and contact junction growth with extended hold periods (e.g., Karner and Marone, 2001; Yasuhara et al., 2005), but this mechanism involves slow rates of change at room temperature, due to the Arrhenius dependency of dissolution and re-precipitation rates on temperature. It is quite possible that welding-induced frictional strengthening is important in volcanic settings due to elevated temperatures. The observed slight apparent strengthening of the water-saturated sample may be a consequence of imperfect saturation or the development of stabilizing negative pore fluid pressures resulting from small magnitudes of dilation in the sample.

A common characteristic of volcanic sediments is that it may weather into clay rich material over time. This is an important consideration with regard to frictional strength because increasing the clay content of a sheared material can dramatically reduce frictional strength (Voight et al., 2002; Saffer and Marone, 2003; Ikari et al., 2007). In the study by Voight et al. (2002), a clay rich sample of volcanoclastic material from the SHV exhibited an extremely low residual friction coefficient of 0.05. Though not explicitly studied in the experiments presented here, it is reasonable to conclude that increasingly weathered volcanic deposits may become frictionally weaker over time.

The behavior exhibited by pre-loaded sediments in our experiments is more or less typical (Lambe and Whitman, 1969; Das, 2002). The denser a granular sample is prior to the onset of shear, the higher the resulting peak strength (Lambe and Whitman, 1969 page 146). Pre-loading can build lateral stresses into a deposit or test sample that are not fully relaxed when the loading is removed or reduced. This behavior in pre-loading may be an important factor in controlling the style of failure of slopes comprised of similar volcanic materials, where stress history and progressive failure may be an important mode of time-dependent collapse. A simple example of a naturally-occurring over-compacted material is that of a pyroclastic flow that is emplaced in a dry state under relatively high normal load,

and then water saturated. The pyroclastic material will be initially compacted in the presence of the high normal load, but when saturated, the material will have reduced effective stress at depth, thereby creating an effectively over-compacted sediment that could have an anomalously high strength.

Because of the small grain-sizes used in our experiments, the measured coefficients of internal friction, and their evolution with strain rates, are anticipated to be broadly representative of volcanic material in the initial stages of failure. We have not considered the complicating effects of elevated pore pressures, partial saturation, elevated temperature, or grain welding.

The initial porosity as measured in our experiments (pre-shear and after applying normal load) has considerable bearing on the presence or absence of a peak in shear strength (e.g., Lambe and Whitman, 1969). For a relatively dense specimen, with a high value for D_r , the curve of shear stress versus displacement shows a pronounced peak (and dilation), and the shear stress decreases following the peak. For a loose specimen, with low D_r , no peak is shown, and the sample strain — hardens to a residual stress that remains essentially constant with further shearing. Our data are consistent with ideas based on critical state porosity, where at any given confining stress and in the absence of grain crushing, a granular material will have a preferred steady-state porosity during shear deformation. A dense specimen will increase in porosity to reach the critical state, and a loose specimen will compact to reach the critical state. Thus the absolute porosity values themselves do not directly indicate whether a material is loose or dense, and porosity values cannot be directly compared from one material to another without also considering the grain-size distribution and grain shape. Predictions of strength evolution are obtained only by comparing the porosity of a given material sample with that of the same material in its loosest and densest possible states. This is expressed by the term relative density in geomechanics, values of which are given in Table 1. We discuss our method of determining the maximum and minimum density in Appendix A. However we note that the standard procedure for this test may be strongly influenced by the small value of normal load used. Thus with the normal loads of 0.75–8 MPa as used in our tests, initial relative densities almost invariably exceeded 100%. A corollary issue is, that despite these large apparent relative densities (implying very dense packing), strength peaks were not invariably seen. These issues are incompletely understood and require further research.

In our tests, peaks in shear strength are commonly observed when initial $D_r \geq 150\%$, which indicates a very dense sample state. Peaks were always observed when the sample was pre-loaded. However the presence or absence of peaks appears random when the initial relative density is <150 , which likely indicates inaccuracies in determining D_r . Initial relative density shows no discernable trend associated with normal stress in our tests, apart from the 0–1 mm SHV samples, where an increased relative density characterizes the 8 MPa test samples. This is potentially due to inconsistency in sample preparation or inadequacies in our technique of porosity measurement.

Experiments conducted at shearing velocities of 10, 100, and 900 mm/s showed a velocity strengthening trend, suggesting that the material would be incapable of hosting unstable stick-

slip sliding. In previous work, gouge material collected from the perimeter of a dacite plug at Mount St. Helens showed velocity weakening behavior (Iverson et al., 2007; Moore et al., 2007). These studies employed a different type of test apparatus and suggested that stick-slip motion of the plug was consistent with observed seismicity. Our results imply that gouge material surrounding a plug in the throat of the Soufrière Hills volcano would likely fail via stable creep rather than by stick-slip motion. However rapid weakening immediately after attainment of a peak strength could lead to instability and other factors, not studied in our experiments, can also be involved. Additional experiments are necessary to fully understand stick-slip and instability in volcanic materials.

6. Conclusions

Based on these experiments we conclude the following:

- 1) Changing the grain-size range of the pyroclastic material tested had only a small effect on the coefficient of residual internal friction. The effect on peak strength also seems small although our test data are few. Possibly this reflects the limited differences between these size ranges with maximum clast size < 1 mm. Also, grain fracture during shearing can reduce the differences between grain-size ranges for samples, resulting in more uniform ranges.
- 2) The saturation of pyroclastic debris recovered from Soufrière Hills results in only a very small increase in the apparent value of internal friction. We cannot exclude the possibility that this effect could result from imperfect initial saturation, or the development of small negative pore fluid pressures with shear induced dilation. The main conclusion is that the coefficient of residual friction for volcanic debris changes very little, if at all, as a result of water saturation.
- 3) Increasing shear velocity has a small but clear strengthening effect on the coefficient on residual internal friction, which increases with slip velocity from 0.62 at 10 $\mu\text{m/s}$, to 0.64 at 100 $\mu\text{m/s}$, 0.65 at 900 $\mu\text{m/s}$. This result suggests that the tested SHV pyroclastic material is incapable of hosting unstable stick-slip motion unless additional factors are involved.
- 4) The samples from broadly dispersed geographical regions (SHV, MSH, and Stromboli) and different provenance and mineralogical compositions, exhibit surprisingly uniform residual and peak frictional characteristics. For the normal stress range from 0.75–8 MPa, the coefficients of residual internal friction varied only in the range 0.61–0.63. The peak friction values for pre-loaded materials could be as high as 0.76–0.80, although this topic has been explored only in preliminary fashion. The peak strengths will also vary as a function of relative density, but this topic has not yet been treated adequately with respect to strength tests on these materials.
- 5) Absolute porosity values do not directly indicate whether a granular material is actually loose or dense. The key information can be obtained only by comparing the porosity of a given material sample with that of the same material in its loosest and densest possible states, as expressed by the term relative density. However we note that the standard procedure for this test may be strongly influenced by the small value of

normal load used, in comparison with stresses of geological interest. Thus with the normal loads of 0.75–8 MPa used in our tests, initial relative densities almost invariably exceeded 100%, and yet, despite this indication of very high relative density, strength peaks were not invariably seen in shear tests. These issues are incompletely understood and require further research.

Acknowledgements

This work was funded by NSF grants EAR-0337627, EAR-0196570, and EAR-0345813 (to CJM), and EAR-05-07324 and EAR-04-08709 (to BV). BV wishes to thank colleagues at the Montserrat Volcano Observatory, the US Geological Survey, and the Italian Dipartimento Protezione Civile Nazionale, for the assistance and helicopter support in carrying out deposit studies and sampling. We thank N.R. Iverson, and J.K. Morgan for the insightful comments, which improved the manuscript.

Appendix A. — relative density measurement

We measured the maximum and minimum density of the experimental materials using ASTM Test Designation D-2049 (Das, 2002) as a general guide. Measurements were made for the SHV pyroclastic materials with gradations 0–1 mm, 0.125–1 mm, 0.063–0.125 mm, 0.5–1 mm; the MSH lahar material 0–1 mm; and Stromboli pyroclastic material 0–1 mm. Three measurements were conducted from each experimental sample and maximum/minimum porosity, maximum/minimum void ratio, and maximum/minimum dry density values were calculated (Table A1). Grain density of the material was measured using a simple volume displacement method.

Measurement of the maximum porosity was made by filling a 28.5 mm I.D., 50 mL graduated cylinder with granular material packed in as loose a state as possible. This was accomplished by using a Pyrex funnel with a 4.5 mm diameter opening, and maintaining an approximately 25 mm drop from the end of the funnel to the top of the gently accumulating sediment fill. The mass of the graduated cylinder was measured before and after it was filled with sediment to obtain the sediment mass, and density of the material was calculated for this loosest packed state.

Once the minimum density had been calculated, material was compacted using a 27.5 mm diameter weight with a mass of 1014 g fitted on top of the granular material inside of the graduated cylinder. This mass corresponds to a pressure of approximately 2.4 lbf/in² (0.017 MPa), which is slightly higher than the 2.0 lbf/in² (0.013 MPa) recommended in ASTM Test D-2049. The graduated cylinder was then vibrated by tapping the side of it with a metal ruler at a frequency of ~3–5 Hz for 8 min. ASTM D-2049 advocates the usage of a vibration table running at 60 Hz for compacting the sediment.

Relative density, D_r , was calculated for the pre-shear void ratio in our experiments using the equation

$$D_r = \frac{(e_{\max} - e)}{(e_{\max} - e_{\min})} \times 100\%, \quad (\text{A1})$$

where e is pre-shear void ratio, and e_{\min} and e_{\max} are respectively the minimum and maximum void ratio as described

Table A1

Measurements of the maximum/minimum dry density, maximum/minimum porosity, maximum/minimum void ratio, made using a test similar to ASTM test designation D-2049 (1999)

Material	Test #	Mineral density (g/cm ³)	Minimum density (g/cm ³)	Maximum density (g/cm ³)	Maximum porosity	Minimum porosity	Maximum void ratio	Minimum void ratio
SHV (0–1 mm)	1	2.7	1.37	1.91	0.49	0.29	0.97	0.41
	2	2.7	1.39	1.93	0.49	0.29	0.95	0.40
	3	2.7	1.37	1.90	0.49	0.30	0.97	0.42
		Average =	1.38	1.91	0.49	0.29	0.96	0.41
		SD =	9.77E–03	1.36E–02	3.62E–03	5.02E–03	1.39E–02	9.98E–03
MSH (0–1 mm)	1	2.52	1.35	1.88	0.46	0.25	0.86	0.34
	2	2.52	1.35	1.88	0.46	0.26	0.86	0.34
	3	2.52	1.36	1.84	0.46	0.27	0.85	0.37
		Average =	1.35	1.86	0.46	0.26	0.86	0.35
		SD =	3.94E–03	2.42E–02	1.56E–03	9.60E–03	5.40E–03	1.77E–02
Stromboli (0–1 mm)	1	2.79	1.57	1.71	0.44	0.39	0.77	0.63
	2	2.79	1.62	1.74	0.42	0.38	0.73	0.61
	3	2.79	1.57	1.72	0.44	0.38	0.78	0.62
		Average =	1.59	1.72	0.43	0.38	0.76	0.62
		SD =	2.67E–02	1.35E–02	9.58E–03	4.83E–03	2.94E–02	1.26E–02
SHV (0.063–0.125 mm)	1	2.66	1.18	1.44	0.56	0.46	1.25	0.85
	2	2.66	1.19	1.45	0.55	0.46	1.24	0.84
	3	2.66	1.17	1.44	0.56	0.46	1.28	0.85
		Average =	1.18	1.44	0.56	0.46	1.26	0.84
		SD =	1.05E–02	4.59E–03	3.95E–03	1.72E–03	2.01E–02	5.84E–03
SHV (0.5–1 mm)	1	2.7	1.45	1.57	0.46	0.42	0.87	0.72
	2	2.7	1.44	1.54	0.47	0.43	0.87	0.76
	3	2.7	1.35	1.52	0.50	0.44	1.00	0.78
		Average =	1.41	1.54	0.48	0.43	0.91	0.75
		SD =	5.55E–02	2.81E–02	2.06E–02	1.04E–02	7.69E–02	3.18E–02
SHV (0.125–1 mm)	1	2.7	1.47	1.67	0.45	0.38	0.83	0.61
	2	2.7	1.41	1.66	0.48	0.39	0.92	0.63
	3	2.7	1.40	1.65	0.48	0.39	0.92	0.64
		Average =	1.43	1.66	0.47	0.39	0.89	0.63
		SD =	3.79E–02	1.10E–02	1.40E–02	4.06E–03	4.95E–02	1.07E–02

Measurements were made using the natural grain-size distribution of the SHV pyroclastic material (<1 mm), MSH lahar, and Stromboli pyroclastic materials as well as restricted grain-size ranges of the SHV material from 0.063–0.125 mm, 0.5–1 mm, and 0.125–1 mm. Shaded regions are the average and standard deviation of three measurements made of each material

previously, and shown in Table A1. Note, porosity n converts to void ratio, by $e=n/(1-n)$. Measurements of pre-shear relative density are given in Table 1.

References

- Anthony, J.L., Marone, C., 2005. Influence of particle characteristics on granular friction. *Journal of Geophysical Research* 110, B08409. doi:10.1029/2004B003399.
- Apuani, T., Corazzato, C., Cancelli, A., Tibaldi, A., 2005. Physical and mechanical properties of rock masses at Stromboli: a dataset for volcano instability evaluation. *Bulletin of Engineering Geology and the Environment* 64 (4), 419–431.
- ASTM Standard D 2049, 1999. Test Method for Relative Density of Cohesionless Soils. ASTM International, West Conshohocken, PA. www.astm.org.
- Bishop, A.W., 1954. Discussion on A.D.M. Penman (1953). *Geotechnique* 4 (1), 43–45.
- Cagnoli, B., Manga, M., 2004. Granular mass flows and Coulomb's friction in shear cell experiments: implication for geophysical flows. *Journal of Geophysical Research* 109, F04005. doi:10.1029/2004JF0001777.
- Das, B.M., 2002. Principles of Geotechnical Engineering. Brooks/Cole, Pacific Grove, CA, 589+xi pp.
- Druitt, T.H., Kokelaar, B.P., 2002. The eruption of Soufrière Hills Volcano, Montserrat, from 1995 to 1999. *Geol. Soc. London, Memoir* vol. 21. 645 pp.
- Guest, J., Cole, P., Duncan, A., Chester, D., 2003. Volcanoes of Southern Italy. The Geological Society, Bath, UK. 284+ix pp.
- Horn, H.M., Deere, D.U., 1962. Frictional characteristics of minerals. *Geotechnique* 12, 319–335.
- Hubbert, M.K., Rubey, W.W., 1959. Role of fluid pressure in mechanics of overthrust faulting. *Bulletin of the Geological Society of America* 70, 115–166.
- Ikari, M.J., Saffer, D.M., Marone, C., 2007. Effect of hydration state on the frictional properties of montmorillonite-based fault gouge. *Journal of Geophysical Research* 112, B06423. doi:10.1029/2006JB004748.
- Inman, D.L., 1952. Measures for describing the size distribution of sediments. *Journal of Sedimentary Petrology* 22 (3), 125–145.

- Iverson, R.M., 1997. The physics of debris flows. *Reviews of Geophysics* 35 (3), 245–296.
- Iverson, R.M., Dzurisin, D., Gardner, C.A., Gerlach, T., LaHusen, R.G., Lisowski, M., Major, J.J., Malone, S.D., Messerich, J.A., Moran, S.C., Pallister, J.S., Qamar, A.I., Schilling, S.P., Vallance, J.W., 2007. Dynamics of seismogenic volcanic extrusion at Mount St Helens in 2004–05. *Nature* 444 (23), 439–443.
- Karner, S.L., Marone, C., 2001. Frictional restrengthening in simulated fault gouge: effect of shear load perturbations. *Journal of Geophysical Research* 106 (B9), 19319–19337. doi:10.1029/2001JB000263.
- Knuth, M., Marone, C., 2007. Friction of sheared granular layers: role of particle dimensionality, surface roughness, and material properties. *Geochemistry Geophysics Geosystems* 8, Q03012. doi:10.1029/2006GC001327.
- Lambe, T.W., Whitman, R.V., 1969. *Soil Mechanics*. Wiley, New York. 553+viii pp.
- Mair, K., Frye, K.M., Marone, C., 2002. Influence of grain characteristics on the friction of granular shear zones. *Journal of Geophysical Research* 107, B102219. doi:10.1029/2001JB000516.
- Mair, K., Marone, C., 1999. Friction of simulated fault gouge for a wide range of velocities and normal stresses. *Journal of Geophysical Research-Solid Earth* 104 (B12), 28899–28914. doi:10.1029/1999JB900279.
- Major, J.J., Iverson, R.M., McTigue, D.F., Macias, S., Fiederowicz, B.K., 1997. Geotechnical properties of debris-flow sediments and slurries. In: Chen, C.L. (Ed.), *Debris-flow Hazards Mitigation. Mechanics, Prediction, and Assessment*. American Society of Civil Engineers, pp. 249–259.
- Marone, C., 1998. Laboratory-derived friction laws and their application to seismic faulting. *Annual Review of Earth and Planetary Sciences* 26, 643–696.
- Marone, C., Kilgore, B., 1993. Scaling of the critical slip distance for seismic faulting with shear strain in fault zones. *Nature* 362 (6241), 618–621.
- Marone, C., Raleigh, C.B., Scholz, C.H., 1990. Frictional behavior and constitutive modeling of simulated fault gouge. *Journal of Geophysical Research* 95 (B5), 7007–7025.
- Marsella, M., Tommasi, I.P., Voight, B., 2004. Monitoring and stability assessment of the Sciarra del Fuoco, Stromboli: the slope stability/tsunami crisis of 28 December 2002–June 2003. *Int. Soc. Volcanol. Chem. Earth's Interior General Assembly (Abstract)*, Pucon, Chile.
- Meyer, W., Sabol, M.A., Glicken, H., Voight, B., 1983. The effects of ground water, slope stability, and seismic hazard on the stability of the South Fork Castle Creek Blockage in the Mount St. Helens Area, Washington. USGS Professional Paper 1250, 1–42.
- Moore, P.L., Iverson, N.R., Iverson, R.M., in press. Frictional properties of the Mount St. Helens gouge, chapter 20 In: Sherrod, D.R., Scott, W.E., Stauffer (Eds.), *A volcano rekindled; the renewed eruption of Mount St. Helens, 2004–2006*. USGS Professional Paper 1750.
- Morgan, J.K., Boettcher, M.S., 1999. Numerical simulations of granular shear zones using the distinct element method 1. Shear zone kinematics and the micromechanics of localization. *Journal of Geophysical research* 104 (B2), 2703–2720.
- Rowe, P.W., 1962. The stress-dilatancy relation for static equilibrium of an assembly of particles in contact. *Proceedings of the Royal Society of London. Series A, Mathematical and Physical Sciences* 269 (1339), 500–527.
- Saffer, D.M., Marone, C., 2003. Comparison of smectite- and illite-rich gouge frictional properties: application to the updip limit of the seismogenic zone along subduction megathrusts. *Earth and Planetary Science Letters* 215, 219–235.
- Scott, D.R., Marone, C.J., Sammis, C.G., 1994. The apparent friction of granular fault gouge in sheared layers. *Journal of Geophysical Research* 99 (B4), 7231–7246.
- Sowers, G.F., 1979. *Introductory Soil Mechanics and Foundations: Geotechnical Engineering*. Macmillan Publishing Co., New York. 621+xvii pp.
- Sowers, G.B., Sowers, B.F., 1951. *Introductory Soil Mechanics and Foundations*. Macmillan Publishing Co., New York. 284+xi pp.
- Terzaghi, K., Peck, R., 1948. *Soil Mechanics in Engineering Practice*. John Wiley & Sons Inc., New York. 566+xviii pp.
- Voight, B. (Ed.), 1976. *Mechanics of Thrust Faults and Decollement*. Dowden, Hutchinson, and Ross, Inc., Stroudsburg PA. 471 pp.
- Voight, B., 2000. Structural stability of andesite volcanoes and lava domes. *Philosophical Transactions of the Royal Society of London. Series A, Mathematical Physical and Engineering Sciences* 358 (1770), 1663–1703.
- Voight, B., Janda, R.J., Glicken, H., Douglass, P.M., 1983. Nature and mechanics of the Mount St Helens rockslide-avalanche of 18 May 1980. *Geotechnique* 33, 243–273.
- Voight, B., Komorowski, J., Norton, G., Belousov, A., Belousova, M., Boudon, G., Francis, P., Franz, W., Heinrich, P., Sparks, R., Young, S., 2002. The 26 December (Boxing Day) 1997 sector collapse and debris avalanche at Soufrière Hills volcano, Montserrat. In: Druitt, T.H., Kokelaar, B.P. (Eds.), *The eruption of Soufrière Hills Volcano, Montserrat, from 1995 to 1999*. *Geol. Soc. London, Memoir*, vol. 21, pp. 363–407. 645 pp.
- Voight, B., Elsworth, D., 1997. Failure of volcano slopes. *Geotechnique* 47 (1), 1–31.
- Voight, B., Elsworth, D., 2000. Instability and collapse of hazardous gas-pressurized lava domes. *Geophysical Research Letters* 27 (1), 1–4.
- Walker, G.P.L., 1971. Grain-size characteristics of pyroclastic deposits. *Journal of Geology* 79, 696–714.
- Watts, R., Herd, R., Sparks, R., Young, S., 2002. Growth patterns and emplacement of the andesitic lavadome and Soufrière Hills Volcano, Montserrat. In: Druitt, T.H., Kokelaar, B.P. (Eds.), *The eruption of Soufrière Hills Volcano, Montserrat, from 1995 to 1999*. *Geol. Soc. London, Memoir*, vol. 21, pp. 115–152. 645 pp.
- Wiebe, B., Graham, J., Tang, G.X.M., Dixon, D., 1998. Influence of pressure, saturation, and temperature on the behaviour of unsaturated sand-bentonite. *Canadian Geotechnical Journal* 35 (2), 194–205.
- Yasuhara, H., Marone, C., Elsworth, D., 2005. Fault zone restrengthening and frictional healing: the role of pressure solution. *Journal of Geophysical Research — Solid Earth* 110, B06310. doi:10.1029/2004JB003327.